

# An approach toward the laboratory search for the scalar field as a candidate of Dark Energy

Yasunori FUJII<sup>a</sup> and Kensuke HOMMA<sup>b,c</sup>

<sup>a</sup> *Advanced Research Institute for Science and Engineering, Waseda University, Okubo, Tokyo, 169-8555 Japan*

<sup>b</sup> *Graduate School of Science, Hiroshima University, Japan, Higashi-Hiroshima 739-8526, Japan*

<sup>c</sup> *Ludwig-Maximilians-Universität München, Fakultät f. Physik, Am Coulombwall 1, D-85748, Germany*

The observed accelerating universe indicates the presence of Dark Energy which is probably interpreted in terms of an extremely light gravitational scalar field. We suggest a way to probe this scalar field which contributes to optical light-by-light scattering through the resonance in the quasi-parallel collision geometry. As we find, the frequency-shifted photons with the specifically chosen polarization state can be a distinct signature of the scalar-field-exchange process in spite of the extremely narrow width due to the gravitationally weak coupling to photons. Main emphasis will be placed in formulating a prototype theoretical approach, then showing how the weak signals from the gravitational coupling are enhanced by other non-gravitational effects at work in laser experiments.

## §1. Introduction

The discovery of the accelerating universe<sup>1)</sup> left today's version of the cosmological constant problem, mainly consisting of a pair of questions; the fine-tuning problem and the coincidence problem. Most promising to understand them appears to introduce a scalar field,<sup>2)-4)</sup> particularly in accordance with the way of Jordan's scalar-tensor theory (STT),<sup>5)</sup> one of the best-known alternatives to Einstein's General Relativity. We add a cosmological constant  $\Lambda$  as a new ingredient, technically in the so-called Jordan (conformal) frame. Unlike in any other approaches, we then derive the scenario of a decaying cosmological constant in the Einstein frame corresponding to the observation;<sup>1)</sup>  $\Lambda_{\text{obs}} \sim t^{-2}$ , where the present age of the universe  $t_0 = 1.37 \times 10^{10} \text{y}$  is re-expressed as  $\sim 10^{60}$  in the reduced Planckian units with  $c = \hbar = M_{\text{P}} (= (8\pi G)^{-1/2} \sim 10^{27} \text{eV}) = 1$ . Given the unification-oriented expectation  $\Lambda \sim 1$  in these units, the decaying behavior provides us with the way of understanding naturally why the observed value is as small as  $10^{-120}$ . The resulting number is this small only because we are *old* cosmologically *not* because we fine-tune any of the theoretical parameters. For more details see the Refs.<sup>3),6)-9)</sup>

The scalar field, denoted by  $\phi$ ,<sup>2)</sup> in STT is then expected to fill up nearly 3/4 of the entire cosmological energy,<sup>1)</sup> known as Dark Energy (DE). In addition to this aspect in which the scalar field plays a major role in the evolution of the entire universe, it also mediates a force between local objects. Unlike the former, the latter component behaves in accordance with the relativistic quantum field theory on the local tangential Minkowski spacetime, now

<sup>1)</sup> This relation implies an *overall* behavior of the effective  $\Lambda$ , superimposed on which we expect *local* plateaus occurring sporadically, hence mimicking *constants* during certain duration of time, as illustrated in Fig. 5.8 of.<sup>3)</sup>

<sup>2)</sup> We are going to use the symbol  $\phi$  for the canonical scalar field in the Einstein frame, rather than in the Jordan frame; different ways in<sup>3)</sup> in which  $\phi$  and  $\sigma$  represent the scalar fields in the Jordan and the Einstein frames, respectively.

suggesting an experimental way to search for it.

It couples with other microscopic fields basically as weakly as gravity. It also shows no immunity against acquiring a nonzero mass due to the self-energy, unlike genuine gauge fields like photon and graviton. A simple one-loop diagram in which the light quarks and leptons with a typical mass  $m_q \sim \text{MeV}$  couple to the scalar field with the gravitational coupling with the strength  $\sim M_{\text{P}}^{-1}$  produces the mass  $m_\phi$  given by

$$m_\phi^2 \sim \frac{m_q^2 M_{\text{ssb}}^2}{M_{\text{P}}^2} \sim (10^{-9} \text{eV})^2, \quad (1.1)$$

where we have included the effective cutoff coming from the super-symmetry-breaking mass-scale  $M_{\text{ssb}} \sim \text{TeV}$ , though allowing a latitude of the few orders of magnitude. The force-range turns out to be  $m_\phi^{-1}$  which has a macroscopic size  $\sim 100\text{m}$ .<sup>3),10)</sup>

Past searches for the scalar force of this kind have been plagued by its matter coupling basically as weak as gravity, hence calling often for heavy and huge objects, sometimes even natural environments, including reservoirs, bore holes, polar ice and so on, with so many uncontrollable uncertainties.<sup>11)</sup> This blockade can be avoided, however, by appreciating that certain scattering amplitude in which  $\phi$  occurs as a resonance reaches a kinematical maximum independent of the interaction strength. The question is, however, what scattering system accommodates  $\phi$  as light as above. We may focus upon the 2-photon system as the most convenient candidate. We also point out that STT allows  $\phi$  to couple to the photons only at the cost of violating the weak equivalence principle (WEP),<sup>12)</sup> though without offending the core of spacetime geometry in General Relativity.<sup>3</sup> We must confront, at the same time, the resonance width which should be very narrow if the coupling is gravitationally weak.

Through detailed study of the two-photon dynamics in which the photon-photon scattering amplitude is dominated by the  $\phi$ -resonance to a very good approximation, to be referred to as  *$\phi$ -resonance-dominance*, we are going to outline how we can enhance the gravitationally weak signals by non-gravitational effects, described in terms of a few number of steps each of which is highly nontrivial, including the recent achievements of laser technology.

We also point out that our approach is somewhat similar to the axion search<sup>13)</sup> in which the pseudoscalar field is produced in the real state rather than in the virtual state. In the present article, however, we attempt detailed discussion on wider aspects of the scattering system, including the physical effects of a narrow resonance, angular distribution, particularly the behaviors in the extremely forward direction .

## §2. Kinematics

For the reasons to be explained shortly, we prefer a special coordinate frame, as shown in Fig.1, in which two photons labeled by 1 and 2 sharing the same frequency are incident nearly parallel to each other, making a small angle  $\vartheta$  with a common central line along the  $z$  axis. In this *quasi-parallel frame*, we define the  $zx$  plane formed by  $\vec{p}_1$  and  $\vec{p}_2$ , with the components of the 4-momenta  $p_1 = (\omega \sin \vartheta, 0, \omega \cos \vartheta; \omega)$  and  $p_2 = (-\omega \sin \vartheta, 0, \omega \cos \vartheta; \omega)$ .

The outgoing photons are assumed to be in the same  $zx$  plane, to be convenient particularly in the  $s$ -channel reaction, showing an axial symmetry with respect to the  $z$  axis;  $p_3 = (\omega_3 \sin \theta_3, 0, \omega_3 \cos \theta_3; \omega_3)$ ,  $p_4 = (-\omega_4 \sin \theta_4, 0, \omega_4 \cos \theta_4; \omega_4)$ . The angles  $\theta_3$  and  $\theta_4$ , both positive  $< \pi$ , are defined also in Fig.1. This coordinate frame is reached by transforming the conventional center-of-mass frame for the head-on collision in the  $x$  direction by a Lorentz

---

<sup>3</sup> The reader is advised to consult Chapter 1.3.1 of.<sup>3)</sup>

transformation with the velocity in the  $z$  direction of the magnitude  $c \cos \vartheta$  with the velocity of light  $c$ .

The conservation laws are

$$0\text{-axis} : \omega_3 + \omega_4 = 2\omega, \quad (2.1)$$

$$z\text{-axis} : \omega_3 \cos \theta_3 + \omega_4 \cos \theta_4 = 2\omega \cos \vartheta, \quad (2.2)$$

$$x\text{-axis} : \omega_3 \sin \theta_3 = \omega_4 \sin \theta_4. \quad (2.3)$$

For a convenient ordering  $0 < \omega_4 < \omega_3 < 2\omega$ , we may choose  $0 < \theta_3 < \vartheta < \theta_4 < \pi$ , without loss of generality. From (2.1)-(2.3) we derive

$$\frac{\sin \theta_3}{\sin \theta_4} = \frac{\sin^2 \vartheta}{1 - 2 \cos \vartheta \cos \theta_4 + \cos^2 \vartheta}. \quad (2.4)$$

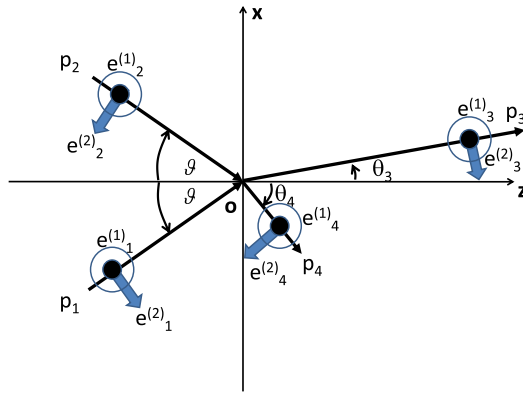


Fig. 1. Definitions of kinematical variables.

The differential elastic scattering cross section favoring the higher photon energy  $\omega_3$  is given by

$$\frac{d\sigma}{d\Omega_3} = \left( \frac{1}{8\pi\omega} \right)^2 \sin^{-4} \vartheta \left( \frac{\omega_3}{2\omega} \right)^2 |\mathcal{M}|^2, \quad (2.5)$$

where  $\mathcal{M}$  is the invariant amplitude, and

$$\omega_3 = \frac{\omega \sin^2 \vartheta}{1 - \cos \vartheta \cos \theta_3}, \quad (2.6)$$

which shows  $\omega_3$  reaching up to  $2\omega$  as  $\theta_3 \rightarrow 0$ , as shown in Fig. 2. In other words, we have a sharp peak of the frequency-doubled final photon with  $\omega_3 \approx 2\omega$ , the total energy, in the extremely forward direction concentrated in  $\theta_3 \lesssim \vartheta$ , or the half-width  $\vartheta$ . This is certainly a unique observational signature.

We point out that the factor  $\sin^{-2} \vartheta$  in (2.5) is derived in computing the phase-volume of the two photons in the final state, as explained in Appendix A, while another same factor comes from the inverse of the flux  $\sqrt{(p_1 p_2)^2} \approx 2\omega^2 \sin^2 \vartheta$  in the photon-photon scattering state in the quasi-parallel frame, as will be discussed in Appendix E. As we will later discuss, the angle  $\vartheta$  is going to be given by  $\vartheta \sim m_\phi/\omega \sim 10^{-9}$  for  $\omega \sim \omega_1 (= 1\text{eV chosen conveniently for the typical optical laser frequency})$ .<sup>4</sup> Out of the huge number  $\sin^{-4} \vartheta \sim \vartheta^{-4}$  as large as  $\sim 10^{36}$ ,

<sup>4</sup> The symbol  $\omega_1$  will be used repeatedly as a frequency (or the energy in the units with  $c = \hbar = 1$ ) of this *value*.

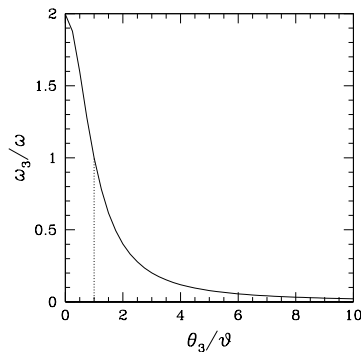


Fig. 2.  $\omega_3/\omega$  plotted against  $\theta_3/\vartheta$ . Note that the forward peak is extremely narrow with the angular width  $\sim \vartheta \sim 10^{-9}$ .

a “half”  $\sim 10^{18}$  does indeed compensate the gravitationally small number  $\sqrt{m_\phi/M_{\text{P}}} \sim 10^{-18}$ . Unfortunately, however, another “half” of this trove will be lost because the final yield is reduced by the ratio of  $\vartheta^2$  when we try to measure the small amount of outgoing photons of nearly doubled frequency in the extremely forward direction. We still maintain a non-trivial gain in the efforts for overcoming the gravitationally weak signals.

In this connection we find it important to point out that there is a decisive difference between the quasi-parallel incident direction corresponding to  $\vartheta \sim 10^{-9}$  and the truly parallel incident beams with  $\vartheta = 0$ . In the lowest-order QED calculation,<sup>14)</sup> the gauge invariance of the theory results in the cross section which vanishes in the limit  $\vartheta \rightarrow 0$ . The same results are also shared in our scalar-field dynamics, as will be explained later toward the end of section 3. In this context, the negative-power dependence on  $\vartheta$  as in (2.5), for example, can be still useful for finite  $\vartheta$  in the transitional range before reaching the truly parallel limit.

### §3. Dynamics

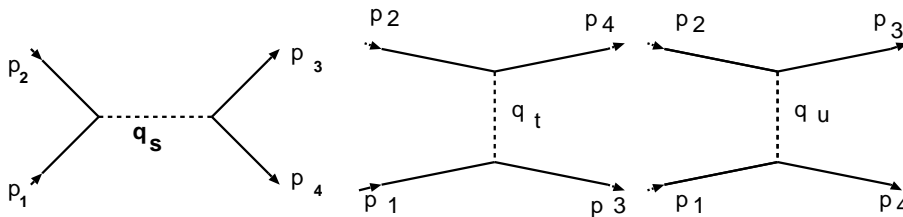


Fig. 3.  $\phi$ -dominated diagrams for the photon-photon scattering. Solid lines are for the photons with the attached momenta  $p$ 's while the dashed lines for  $\phi$ , in the  $s$ -,  $t$ -, and  $u$ -channels, respectively.

We assume the tree diagrams illustrated in Fig. 3, with the vertices given by the  $\phi$ -photon coupling described by the effective interaction Lagrangian;

$$-L_{\text{mx}\phi} = \frac{1}{4} B M_{\text{P}}^{-1} F_{\mu\nu} F^{\mu\nu} \phi, \quad (3.1)$$

where, due to the quantum-anomaly-type estimate,  $B = (2\alpha/3\pi)\mathcal{Z}\zeta$ .<sup>3) 5</sup> Note that the coupling constant  $\sim M_{\text{P}}^{-1} \sim G^{1/2}$  implies being *weak* gravitationally. The above interaction

<sup>5</sup> The coefficient (1/12) in (6.181) in<sup>3)</sup> has been multiplied by 4 when the complex scalar matter fields in

term, which has been discussed also from a phenomenological point of view,<sup>15)</sup> is WEP violating,<sup>12)6)</sup> already against Brans-Dicke's premise.<sup>16)</sup>

We find, for example,

$$\langle 0 | F_{\mu\nu} | p_1, e_1^{(\beta)} \rangle = i \left( p_{1\mu} e_{1\nu}^{(\beta)} - p_{1\nu} e_{1\mu}^{(\beta)} \right), \quad (3.2)$$

giving the two-photon decay rate of  $\phi$  with the mass  $m_\phi$ ;

$$\Gamma_\phi = (16\pi)^{-1} (BM_{\text{P}}^{-1})^2 m_\phi^3, \quad (3.3)$$

by assuming purely elastic scattering. We find the lifetime  $\tau_\phi = \Gamma_\phi^{-1}$  to be as long as  $\sim 3 \times 10^{54}$  times the present age of the universe.

The polarization vectors are given by  $\vec{e}_i^{(\beta)}$  with  $i = 1, \dots, 4$  for the photon labels, whereas  $\beta = 1, 2$  are for the kind of the linear polarization, also shown in Fig.1.

In the  $s$ -channel, as illustrated in the first diagram in Fig. 3, the scalar field is exchanged between the pairs  $(p_1, p_2)$  and  $(p_3, p_4)$ , thus giving the squared momentum of the scalar field  $q_s^2 = (p_1 + p_2)^2 = 2\omega^2 (\cos 2\vartheta - 1) < 0$  with the metric convention  $(+ + + -)$ .

With the type  $\beta = 1$  for all the photons we find;<sup>7)</sup>

$$\mathcal{M}_{1111s} = -(BM_{\text{P}}^{-1})^2 \frac{\omega^4 (\cos 2\vartheta - 1)^2}{2\omega^2 (\cos 2\vartheta - 1) + m_\phi^2}, \quad (3.4)$$

also with  $\mathcal{M}_{1111s} = \mathcal{M}_{2222s} = -\mathcal{M}_{1122s} = -\mathcal{M}_{2211s}$  for the only nonzero components.

It immediately follows that the denominator, the propagator of  $\phi$ , vanishes at

$$\omega^2 = \omega_r^2 \equiv \frac{m_\phi^2/2}{1 - \cos 2\vartheta}, \quad (3.5)$$

corresponding to the creation of the scalar field  $\phi$ . Note that with the assumed value of  $m_\phi \sim 10^{-9}$  eV, we find that  $\omega_r$  can be as large as  $\sim \omega_1 = 1$  eV by choosing  $\vartheta \sim 10^{-9}$ , as alluded before.<sup>8)</sup>

At the same time the decay rate (3.3) suggests that the propagator acquires an imaginary part obtained approximately by the replacement;  $m_\phi^2 \rightarrow (m_\phi - i\Gamma_\phi/2)^2 \approx m_\phi^2 - im_\phi\Gamma_\phi$ . We may then find that the denominator, denoted by  $\mathcal{D}$ , can be re-expressed as

$$\mathcal{D} \approx 2(1 - \cos 2\vartheta)(\chi + ia), \quad \text{with} \quad \chi = \omega^2 - \omega_r^2, \quad (3.6)$$

where

$$a = \frac{m_\phi\Gamma_\phi/2}{1 - \cos 2\vartheta}. \quad (3.7)$$

---

the loop in the toy model are replaced by the more realistic Dirac fields.  $\zeta$  is a constant of the order unity, while  $\mathcal{Z} = 5$  is the effective number of the fundamental charged particles in the loop, quarks and leptons, actually the sum of their squared charges but re-normalized in units of the standard electron charge squared.

<sup>6)</sup> This failure of WEP is a typical quantum effect, thus causing the true physical frame being slightly off the pure Einstein frame, hence producing two kinds of consequences: (i) non-Newtonian-type interactions, discussed in Chapter 6.4 of;<sup>3)</sup> (ii) the electron mass which provides with the Bohr radius and the atomic-clock frequency is maintained constant in the Einstein frame to a good approximation, in practice, to observe Own-unit-insensitivity principle.<sup>7)</sup>

<sup>7)</sup> The four digits in the subscript are for  $\beta$  arranged from left to right according to the photon labels, 1-4.

<sup>8)</sup> This relation may also be interpreted that the quasi-parallel frame provides us with a device that *lowers* the center-of-mass energy to the invariant mass  $m_\phi$  by choosing  $\vartheta$  small enough for given  $\omega$ .

Choosing  $\vartheta \sim 10^{-9}$ , also combining again with (3.3), we find  $a \sim 10^{-77}(\text{eV})^2$ , which will be used later repeatedly.

The amplitude (3.4) can be further re-expressed by the Breit-Wigner formula. To show this explicitly, we denote the portion of (3.4) other than  $\mathcal{D}$  by  $\mathcal{N}$  evaluated at  $\omega_r$ ;

$$\mathcal{N} \approx (BM_{\text{P}}^{-1})^2 \omega_r^4 (1 - \cos 2\vartheta)^2. \quad (3.8)$$

We compare this with (3.3), eliminating the common factor  $(BM_{\text{P}}^{-1})^2$ , to obtain

$$\mathcal{N} \approx 16\pi\Gamma_\phi m_\phi^{-3} \omega_r^4 (1 - \cos 2\vartheta)^2 = 4\pi\Gamma_\phi m_\phi = 8\pi a (1 - \cos 2\vartheta), \quad (3.9)$$

where we have used (3.5) and (3.7) in the second and the last steps, respectively. From this and (3.6), we finally obtain

$$\mathcal{M}_{1111s} = \frac{\mathcal{N}}{\mathcal{D}} \approx 4\pi \frac{a}{\chi + ia}, \quad \text{hence} \quad |\mathcal{M}_{1111s}|^2 \approx (4\pi)^2 \frac{a^2}{\chi^2 + a^2}. \quad (3.10)$$

At the resonance position  $\omega = \omega_r$  or  $\chi = 0$ , we find  $\mathcal{M}_{1111s} = -4\pi i$  or  $|\mathcal{M}_{1111s}|^2 = (4\pi)^2$ , a ‘‘large’’ value entirely free from being small for a gravitational force. This obvious result due directly to the element of quantum mechanics is the heart of what we may call  $\phi$ -dominance, as was pointed out in section 1. In fact without this resonance we would have found  $|\mathcal{M}|^2$  to be as small as  $M_{\text{P}}^{-4}$  either directly from the diagram due to (3.1) or from the numerator  $a^2$  in the second of (3.10) again combined with (3.3).

This smallness holds true for the processes in the  $t$ - and  $u$ -channels, as well, with  $q_t$  and  $q_u$  both spacelike, hence no chance of being enhanced due to the resonance. In other words, a resonance occurring only in the  $s$ -channel awards us with a gain of  $\sim M_{\text{P}}^4$ , or of such dimensionless factors like  $(M_{\text{P}}/(\text{eV}))^4 \sim 10^{108}$  or  $(M_{\text{P}}/m_\phi)^4 \sim 10^{144}$  for  $m_\phi \sim 10^{-9}\text{eV}$ . We may take advantage of such huge numbers of this nature in our effort to overcome the weak coupling of gravity, as alluded at the beginning. We face, however, another consequence of the weak coupling resulting in the extremely *narrow* width  $a \sim 10^{-77}(\text{eV})^2$ , implied by  $M_{\text{P}}^{-2}$ , unimaginably small in any practical measurements available currently.

This is even narrower than what is expected from the quantum-theoretical uncertainty of the momenta to be included in any of the existing beams in particle physics. The quasi-parallel frame, as we noted before, requires us to prepare the beam with the accuracy of the angle  $\vartheta \sim 10^{-9}$  to be realized around the focal point in the diffraction limit, where the momentum uncertainty is unavoidable in principle. This seems to present an argument, though never stated before, to be applied carefully to the extreme situation under the present discussion. A natural way to cope with the issue of this fundamental importance is to apply an *averaging* process over the range of the likely uncertainty. More specifically, we integrate the squared amplitude with respect to  $\chi$  uniformly over the range  $\mathcal{R} = (-\tilde{a}, \tilde{a})$ ;

$$\overline{|\mathcal{M}_{1111s}|^2} = \frac{1}{2\tilde{a}} \int_{-\tilde{a}}^{\tilde{a}} |\mathcal{M}_{1111s}|^2 d\chi = (4\pi)^2 \eta^{-1} \frac{\pi}{2} \hat{\eta}. \quad (3.11)$$

The far RHS is obtained immediately by substituting from the second of (3.10), where we assume  $\eta \equiv \tilde{a}/a \gg 1$ , also with  $\hat{\eta} = (2/\pi) \tan^{-1} \eta$ , reaching the maximum 1 for  $\eta \rightarrow \infty$ , while reducing to be negligibly small if the resonance is outside the range  $\mathcal{R}$ . We emphasize that the integral in (3.11) is insensitive to the choice of the integration boundaries, as long as they are much larger than  $a$ . We may also find explicitly how the uncertainty in  $\vartheta$  affects the same in  $\chi$  will be shown shortly in (3.15), for example.

The averaging process proposed in (3.11) has an added advantage, by providing a practical way of measurement of the realistic accuracy of the order  $\sim \text{eV}$ . We also notice that the small number  $\eta^{-1} = a/\tilde{a}$  on the right-hand side of (3.11) simply reflects how small a portion the resonance occupies in the entire range  $\mathcal{R}$ . Part of the gain as large as than  $10^{144}$  emphasized above will thus be offset by  $\eta^{-1}$ . We nevertheless will show that the net result is still sufficiently large. For this purpose, we start with summarizing what we have found so far, by substituting (3.11) into (2.5) yielding the averaged cross section

$$\overline{\left(\frac{d\sigma}{d\Omega_3}\right)}_s = \frac{\pi}{8\omega^2} \left(\frac{\omega_3}{2\omega}\right)^2 \vartheta^{-4} \eta^{-1}, \quad (3.12)$$

where we have put  $\hat{\eta} = 1$ .

We want to relate the boundary value  $\tilde{a}$  somehow to the observations. For this purpose we first notice that in the above analysis it may sound as if we vary the incident frequency  $\omega$  with the angle  $\vartheta$  kept fixed to the value  $\vartheta_1$ , for example, so that, according to (3.5),

$$\omega_r^2 = \frac{m_\phi^2}{4\vartheta_1^2}, \quad (3.13)$$

which is hence fixed. In the process of beam focusing with a laser field, on the contrary, we are led almost to fix  $\omega$  to  $\omega_1 (= 1\text{eV}, \text{ for example})$ , but leaving  $\vartheta$  to vary largely due to the unavoidable nature in the diffraction limit. Then  $\omega_r$  is now a variable expressed as a function of  $\vartheta$  by

$$\omega_r^2 = \frac{m_\phi^2}{4\vartheta^2}. \quad (3.14)$$

Substituting this into the second of (3.6), we obtain

$$\chi(\vartheta) = \omega_1^2 \left(1 - \left(\frac{\vartheta_r}{\vartheta}\right)^2\right), \quad (3.15)$$

where

$$\omega_1^2 = \frac{m_\phi^2}{4\vartheta_r^2}, \quad (3.16)$$

which defines  $\vartheta_r$ .<sup>9</sup>

Suppose the two ends  $\pm\tilde{a}$ , obviously chosen for simplicity, in (3.11) correspond to the two boundary values of the angle  $\vartheta_\pm$ ,

$$\chi(\vartheta_\pm) = \pm\tilde{a}, \quad (3.17)$$

which allows us to express  $\vartheta_-$  in terms of  $\vartheta_+$ , as will be shown in Appendix B, eventually to give the coefficient  $\eta$  which occurs in (3.12);

$$\eta = \left(1 - \left(\frac{\vartheta_r}{\vartheta_+}\right)^2\right) \eta_0, \quad (3.18)$$

where

$$\eta_0 \equiv \frac{\omega_1^2}{a} \sim 10^{77}. \quad (3.19)$$

---

<sup>9</sup> The alternate roles played by  $\omega$  and  $\vartheta$  in this sense indicate a more general situation that they represent two experimental handles of the system. The resonance takes place by satisfying the relation of the type of one of (3.13), (3.14) or (3.16), which define the resonance condition expressed by a *band* in the  $\omega$ - $\vartheta$  plane.

We may identify  $\vartheta_+$  with the observational uncertainty  $\Delta\vartheta$  of the angle  $\vartheta$ . We may reasonably assume  $\vartheta_r \ll \Delta\vartheta$ , to arrive at a simpler result

$$\eta \approx \eta_0, \quad (3.20)$$

indicating  $\tilde{a}$  to be of the size of practical measurements.

As far as the connection with observables are concerned, we may try another average over  $\vartheta$  rather than  $\chi$  in (3.11). As we find in Appendix C, however, the same process over  $\vartheta$  results in

$$\frac{\overline{|\mathcal{M}_{1111s}|^2}}{\overline{|\mathcal{M}_{1111s}|^2}} \approx \frac{\vartheta_r}{\vartheta_+}, \quad (3.21)$$

which implies the  $\vartheta$ -average somewhat smaller than that of the  $\chi$ -average, still within basically of the same order of magnitude as  $\eta_0^{-1}$ .

Before closing this section, we show explicitly that no infinity occurs physically as  $\vartheta \rightarrow 0$ , as alluded at the end of section 2. For this purpose, we first consider the limit in which the  $\vartheta$ -dependent term  $2\omega^2(\cos 2\vartheta - 1) \sim -4\omega^2\vartheta^2$  in the denominator of (3.4) is negligibly smaller than another term of  $m_\phi^2$ . The condition may be expressed as

$$\vartheta^2 \ll \vartheta_r^2 = \frac{m_\phi^2}{4\omega_1^2} \sim (10^{-9})^2, \quad (3.22)$$

where  $\vartheta_r$  satisfies the resonance condition for any choice of  $\omega_1$  in the range of optical frequency  $\sim 1\text{eV}$ . In this limit, we find that the amplitude (3.4) depends on  $\vartheta$  only through the numerator, hence yielding the behavior like  $\vartheta^4$  as  $\vartheta \rightarrow 0$ . It then follows that  $|\mathcal{M}|^2$  behaves like  $\sim \vartheta^8$  which overcancels  $\vartheta^{-4}$  in (2.5), hence, proving the absence of infinities as  $\vartheta \rightarrow 0$ , in conformity with the lowest-order QED calculation. We re-emphasize, however, this occurs for  $\vartheta$  much away from  $\vartheta_r \sim 10^{-9}$ . On the other hand, for  $\vartheta$  close to  $\vartheta_r \sim 10^{-9}$  which is  $\phi$ -resonance-dominance not obeying (3.22), the terms like  $\vartheta^{-4}$  in (2.5) can be simply large but stay finite. This is what we may expect as one of the enhancement mechanisms.

#### §4. An overall enhancement scenario

We are now ready to sketch briefly what we have achieved based on the relation (3.12) with  $\eta \sim \eta_0$  which applies to the simple models of uniform distribution with respect to  $\chi$  to a reasonable accuracy. As we recall, we compare  $|\mathcal{M}|^2 \sim M_P^0$  at the resonance position with  $|\mathcal{M}|^2 \sim M_P^{-4}$  as a whole. This might be represented by a gigantic leap shown near the left end of Fig. 4. This will be followed by a setback by  $\eta \sim 10^{-77}$  occurring corresponding to the averaging processes, required to overcome the narrow width of the resonance. Remarkably enough we are still at the middle, up by more than 70 orders of magnitude from the bottom.

We then naturally wonder if we we further exploit  $\vartheta^{-4} \sim 10^{36}$  in (3.12) for a more gain. Further developing our account at the end of the preceding section, we should scrutinize the extremely sharp peak of the angular distribution of  $\omega_3$  in the forward direction as illustrated in Fig.2. In this connection we are concerned about the noise due to the large amount of non-interacting photons flowing out to the forward direction. One of the ways to remove this is to set up a threshold  $\bar{\omega}_3$ , collecting the desired data by accepting those only with  $\omega_3 > \bar{\omega}_3$  with  $\omega < \bar{\omega}_3 < 2\omega$ .



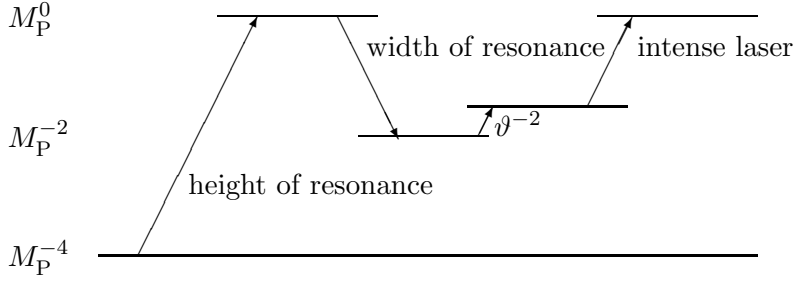


Fig. 4. Schematic representation of enhancing the gravitationally weak signals  $\sim M_{\text{P}}^{-4}$  finally to those at the level of  $\sim M_{\text{P}}^0$ .

By substituting  $\bar{\omega}_3$  into  $\omega_3$  in (2.6), we find the maximum angle  $\bar{\theta}_3$  corresponding to  $\bar{\omega}_3$ ;

$$\underline{x} \equiv \cos \bar{\theta}_3 \approx 1 + \frac{1}{2}\vartheta^2 \left(1 - \frac{2\omega}{\bar{\omega}_3}\right) \approx 1 - \frac{1}{4}\vartheta^2 u, \quad \text{or} \quad \bar{\theta}_3 \approx \vartheta \sqrt{\frac{u}{2}}, \quad (4.1)$$

where the parameter  $u$ , chosen reasonably smaller than 1, is defined by

$$\frac{\bar{\omega}_3}{\omega} = 2 - u. \quad (4.2)$$

Nearly automatically, we are now considering the *partially integrated* cross section defined by

$$\bar{\sigma} = 2\pi \int_0^{\bar{\theta}_3} \left(\frac{d\sigma}{d\Omega_3}\right) \sin \theta_3 d\theta_3. \quad (4.3)$$

In view of the fact that  $\bar{\theta}_3 \lesssim \vartheta$ , as shown by the second of (4.1), much smaller than any angular resolution of ordinary observations, we are making use only of a tiny portion of the available solid angle, which we may prepare in any conventional measurements. Also noticing that the integrand on RHS of (4.3) is likely linear with respect to  $\theta_3$ , we easily expect  $\bar{\sigma}$  is proportional to  $\vartheta^2$ .

The exact value of the coefficient will be determined by

$$\int_0^{\bar{\theta}_3} \left(\frac{\bar{\omega}_3}{2\omega}\right)^2 \sin \theta_3 d\theta_3 \approx \frac{1}{4}\vartheta^2 u. \quad (4.4)$$

Details of estimating LHS, as shown in Appendix D, gives RHS.

Substituting this into (4.3) also from (3.12) we finally obtain

$$\bar{\sigma} \approx \frac{\pi^2}{16\omega^2} \eta^{-1} \vartheta^{-2} u. \quad (4.5)$$

Unlike  $\vartheta^{-4}$  in (3.12), we have now  $\vartheta^{-2} \sim 10^{18}$  as a result of  $\vartheta^2$  in (4.4).

We are still short of somewhere around 60 orders of magnitude before reaching the goal of  $M_{\text{P}}^0$ .

## §5. Enhancement by high-intensity lasers

We now discuss how much we can further enhance the signals by making use of high-intensity laser fields. In order to evaluate the approximate order of magnitude for the required intensity, we consider one of the simplest conceptual setups: a single Gaussian laser beam

with the linearly polarized state  $11$  focused by an ideal lens. Inside this single beam, two photons will scatter each other in the  $s$ -channel most likely in the diffraction limit at around the focal point. A frequency-upshifted photon is emitted nearly in the forward direction in which we may place a prism element to directionally separate the frequency-shifted photons from non-interacting photons followed by a polarization filter to ensure the final state polarization consistent with the scalar field exchange. As for the scalar exchange, in principle, the transitions on the polarization states  $11 \rightarrow 11$  and  $11 \rightarrow 22$  are possible based on (3.4). The requirement of  $11 \rightarrow 22$  should improve the signal to noise ratio against the background from the non-interacting case  $11 \rightarrow 11$  in addition to the requirement of the frequency shift. With many technical arrangements yet to be scrutinized, the simplified concept is still useful to discuss the necessary laser intensity for yielding a sufficient number of frequency-shifted photons.

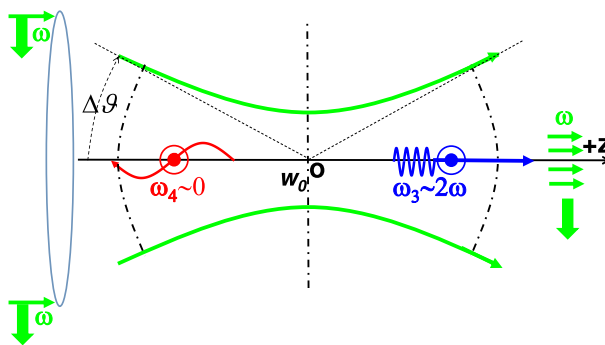


Fig. 5. A single Gaussian laser beam focused by an ideal lens where a scalar field exchange entails a frequency-upshifted photon in the forward direction associated with the transition of the linear polarization state from  $11$  to  $22$ . The frequency of the incident laser beam is assumed to be within a narrow band, while the incident angle varies largely including the value  $\sim 10^{-9}$ .

Let us first consider a luminosity factor per laser pulse duration in an analogy to the concept applied to high-energy collider experiments. A minimum time scale of  $\sim \omega^{-1}$  is considered for interaction within laser pulse duration. We then define the integrated luminosity in this time-scale only in the vicinity of the focal point by

$$\mathcal{L} = \frac{I}{\pi w_0^2}, \quad (5.1)$$

where  $w_0$  is the beam-waist at the focal point, while  $I = N_f(N_f - 1)/2 \sim N_f^2$  is the combinatorics in choosing pairs of incident particles out of the total number  $N_f$  contained in a pulse, or a bunch. This procedure is acceptable when we deal with fermions which are all distinguishable from each other. For bosons, like coherent photons, however, we face a totally different circumstance of a degenerated state in which particles are indistinguishable, hence uncountable. Preparing for the required new formulation, as will be shown, turns out to entail the same intensity factor as in the fermionic particles.<sup>10</sup>

<sup>10</sup> In the following, we show a content somewhat different from section 6 of Ref.,<sup>9)</sup> though basically as a continued outgrowth of the discussion on the inducement mechanism.

On the analogy with fermionic beams, we consider independent two photon-beams which are to be collided to each other, though more realistic experimental setup has been already proposed above. Each of the two laser beams in this simplified case is described, however, by means of the quantized version of the coherent state which features a superposition of different photon numbers, characterized by an *averaged photon number*  $N$ <sup>17)</sup><sup>11</sup>

$$|N \gg \equiv \exp(-N/2) \sum_{n=0}^{\infty} \frac{N^{n/2}}{\sqrt{n!}} |n \rangle, \quad (5.2)$$

where  $|n \rangle$  is the normalized state of  $n$  photons

$$|n \rangle = \frac{1}{\sqrt{n!}} (a^\dagger)^n |0 \rangle, \quad (5.3)$$

with  $a^\dagger$  and  $a$  the creation and the annihilation operators, respectively, of the photons assumed to share a single common frequency and polarization. Admitting that this could be part of an approximation when applied to a pulse laser where multiple frequencies must be included, we still believe it to offer a good starting point to investigate this simplified but well-defined approach. We then derive immediately the normalization condition

$$\ll N |N \gg = 1. \quad (5.4)$$

From (5.2) we derive the relations;<sup>12</sup>

$$a |N \gg = \sqrt{N} |N \gg, \quad \text{and} \quad \ll N | a^\dagger = \sqrt{N} \ll N |, \quad (5.5)$$

where we have made use of the familiar results

$$a^\dagger |n \rangle = \sqrt{n+1} |n+1 \rangle, \quad \text{and} \quad a |n+1 \rangle = \sqrt{n+1} |n \rangle. \quad (5.6)$$

We emphasize that these relations in (5.6) are the basis of what has been known as the *induced* (or stimulated) emission/absorption, or creation/annihilation processes long discussed historically in association with atomic transitions.<sup>13</sup> The simplest choice  $n = 0$  results in the special examples of the *spontaneous* processes.

By combining (5.5) with (5.4) we reach

$$\ll N | a |N \gg = \ll N | a^\dagger |N \gg = \sqrt{N}. \quad (5.7)$$

From (5.5) also follows

$$\ll N | n |N \gg = \ll N | (a^\dagger a) |N \gg = N, \quad (5.8)$$

providing a *posteriori* derivation of the expectation value of  $n$  to be  $N$ .

We expect that the laser beam will enter the system in the form of a coherent state. In order to understand how the coherent state introduced above modifies the conventional Feynman amplitude, we start with re-expressing the one for the first diagram in Fig. 3, with obvious simplifications;

$$V_2 \left( (p_1 + p_2)^2 + m_\phi^2 \right)^{-1} V_1, \quad (5.9)$$

---

<sup>11</sup> Instead of the original complex parameter  $\alpha$ , we use a less general real number  $N = |\alpha|^2$  to simplify the equations shown in the following.

<sup>12</sup> These equations were used in<sup>17)</sup> to *define* a coherent state in the quantum theoretical sense.

<sup>13</sup> See<sup>18)</sup> for a discussion of a possible enhancement effect not necessarily associated with atomic transitions.

where  $V_1$  and  $V_2$  correspond to the matrix elements of the interaction (3.1) at the first and the second vertices, respectively;

$$V_1 = B \langle 0|F_{\mu\nu}|p_1\rangle \langle 0|F^{\mu\nu}|p_2\rangle, \quad \text{and} \quad V_2 = B \langle p_3|F_{\mu\nu}|0\rangle \langle p_4|F^{\mu\nu}|0\rangle. \quad (5.10)$$

For further simplicity, we suppress all the complications arising from the momenta and polarization vectors, finding

$$\langle 0|F_{\mu\nu}|p_1\rangle \rightarrow \langle 0|a|p_1\rangle = 1, \quad (5.11)$$

in the first factor in  $V_1$ , for example, where the second of (5.6) is applied with  $n = 0$ .

The ket  $|p_1\rangle$  implies that we have a one-photon state at the initial time. But this feature should be revised if the photon comes from those embedded in the coherent state prepared before the photons enter the system from the left of the lens, as shown in Fig. 5. The initial state should now be  $|p_1, N\rangle \gg$ , where we exhibit  $p_1$  explicitly for the momenta inside the coherent state, which is also supposed to extend over the region around the first vertex. The photon  $p_1$  reaches here, finding itself surrounded by the sea of photons sharing the same common frequency and polarization as its own, thus annihilates in the induced manner. Correspondingly, the ‘‘final’’ state represented by  $\langle 0|$  in (5.11), the vacuum, is now going to be replaced by  $\ll p_1, N|$ . In this way, the second half of (5.11) is replaced finally by

$$\ll p_1, N|a|p_1, N\rangle \gg = \sqrt{N}, \quad (5.12)$$

precisely the first of (5.7). By comparing this with (5.11) we come to finding that the presence of the coherent state results in an *enhancement* by  $\sqrt{N}$ . Basically the same analysis applies to another incident photon with the momentum  $p_2$ . Summarizing, the presence of the coherent states enhances the matrix element  $V_1$  by  $(\sqrt{N})^2 = N$ . The same result can also be re-interpreted in terms of the enhanced coupling constant  $NB$  at the first vertex.

We now move on to discuss  $V_2$  at the second vertex, in which the outgoing photons are emitted with the momenta  $p_3$  and  $p_4$  most likely quite different from the initial ones, in fact providing us with what we called a unique observational signature as was emphasized in sections 2 and 4. In this sense, the final photons are created spontaneously simply from the vacuum, no enhancement, without the sea of photons provided by the coherent state. Combining this with the foregoing result for the first vertex, we find the total event *rate* for the nearly-doubled frequency  $\omega_3$  to be enhanced effectively by  $((\sqrt{N})^2)^2 = N^2$ .

This result can be re-expressed as in (5.1), in the form of

$$\mathcal{Y} = \frac{I_c}{\pi w_0^2} \bar{\sigma}, \quad (5.13)$$

where

$$I_c = 1 \times N^2, \quad (5.14)$$

which, according faithfully to our derivation, should be understood to be a product of the number (=1) of collision between a pair of coherent states and the coupling strength squared (=  $N^2$ ). It still seems intriguing to find an approximate numerical agreement between  $I_c$  defined by (5.14) and  $I \sim N_f^2$  in (5.1) as long as  $N \sim N_f$ , though they are different from each other conceptually, combinatorics *vs* enhancements due to inducement.<sup>14</sup> See Appendix

<sup>14</sup> The agreement, though approximate and accidental, might instigate an attempt for using combinatorics also applied to the coherent state in terms of the average  $N$ . This might be convenient if we insist that the annihilated photon must have been produced before, as can be implemented by another factor, the second of (5.7). But this not only lacks the responsible interaction, but is also redundant; no need for an ancestor. More important is the absence of the evidence for an overall enhancement  $N^4$  in any of the laser experiments on atoms.

E for a brief account of the mechanism behind deriving (5.13).

Now the uncertainty on the incident angle between two light waves in the single-beam focusing is expected to be

$$\Delta\vartheta \sim \frac{w_0}{z_R} = \pi^{-1} \frac{\lambda}{w_0}, \quad (5.15)$$

from the definition of the Rayleigh length  $z_R \equiv \pi w_0^2/\lambda$  with the optical laser wavelength  $\lambda \sim 10^{-6}$  m.<sup>19)</sup> In principle, we may control  $\Delta\vartheta$  by changing the lens diameter and the focal length. For the assumed diffraction limit  $w_0 \sim \lambda$ , we expect  $\Delta\vartheta \sim \pi^{-1}$ , hence  $\vartheta_r/\vartheta_+ \ll 1$ . In this way, we may assume  $\eta \sim \eta_0$  in (4.5) through the result (3.18) for  $\vartheta_r \ll \Delta\vartheta$ . We then express the number of the expected nearly frequency-doubled photons per pulse focusing  $\mathcal{Y}$  as

$$\mathcal{Y} \sim \frac{u}{64\pi} \vartheta_r^{-2} \eta^{-1} N^2. \quad (5.16)$$

By requiring  $\mathcal{Y} \sim 1$  per pulse focusing, we find the required pulse energy as

$$\bar{N} \sim \left( \frac{64\pi\eta\vartheta_r^2\mathcal{Y}}{u} \right)^{1/2} \sim 10^{31} \text{optical photons} \sim 10^{10} \text{kJ}, \quad (5.17)$$

for  $\omega = 2\pi/\lambda \sim 1\text{eV}$ ,  $u \sim 0.1$ ,  $\eta \sim \eta_0 \sim 10^{77}$ , and  $\vartheta_r \sim 10^{-9}$ . This energy per pulse is far beyond what is presently achievable.

As a rescue, we now wonder if we are allowed to revise the spontaneous nature at the second vertex in which both of the final photons were supposed to be created from the vacuum.<sup>15</sup> We in fact find the desired induced nature realized if we introduce another laser beam again as a coherent state, with its momentum fine-tuned to  $p_4$ , which we may keep fixed within a range specifically in such a way to maintain the nearly-doubled frequency  $\omega_3$  in the forward direction, simply due to the energy-momentum conservation laws. We may consider an experimental setup as illustrated in Fig.6, where  $\omega_4$  with the prescribed energy  $u\omega$  enforces  $\omega_3$  to be  $(2-u)\omega$ . If  $\omega_3$  and  $\omega_4$  are separated largely from each other, we can define  $\omega_3$  as a clear experimental signature by adding the specification of the polarization state consistent with the scalar exchange, because  $\omega_3$  is different from any prescribed laser energies, *i.e.*, neither  $\omega$  nor  $u\omega$ .

The new beam, to be called an *inducing* beam, is chosen to share the same average number  $N$  as before. This beam provides us with a sea of photons from which the photon  $p_4$  is created in the induced manner, so that  $\langle p_4 | F^{\mu\nu} | 0 \rangle$  in the second of (5.10) will be modified to

$$\langle p_4 | a^\dagger | 0 \rangle \rightarrow \ll p_4, N | a^\dagger | p_4, N \gg = \sqrt{N}, \quad (5.18)$$

precisely the time-reversed process of the ones for the incident photons with  $p_1$  and  $p_2$  in  $V_1$ , as in (5.12). Notice that the photon  $p_3$  remains to be created spontaneously from the vacuum because its momentum is quite away from  $p_4$  of the beam.

No attempt is made to observe the photon  $p_4$ , which will be embedded quietly in  $\langle p_4, N |$ . We nevertheless reach a remarkable consequence; detecting the photon  $p_3$  in the unique observational signature as emphasized before, but with the rate enhanced by  $N$ ,

<sup>15</sup> Sometimes the process at the second vertex is called a decaying process (from the scalar field). This might also entail a view that the two photons are the decay products. This may not be entirely inappropriate from a phenomenological point of view. We nevertheless continue to interpret these photons as being created from a field-theoretical point of view. They are created no matter what their origin might be. In this way we maintain a logical consistency with understanding the process taking place at the first vertex in the first of Fig. 3.

because  $\sqrt{N}$  on RHS of (5.18) multiplies the effective coupling strength  $B$  in  $V_2$  in the second of (5.10) at the second vertex. Combining this with the previous enhancement by  $N^2$  arising from the first vertex, we finally find that the net enhancement of the rate of the signal is  $N^3$  which replaces  $N^2$  in (5.16). This implies that the exponent  $1/2$  on the middle of (5.17) is now replaced by  $1/3$ . This entails  $\sim 10^{21}$  optical photons  $\sim 1\text{kJ}$  on its RHS for the required pulse energy, fortunately achievable within the current laser technology.

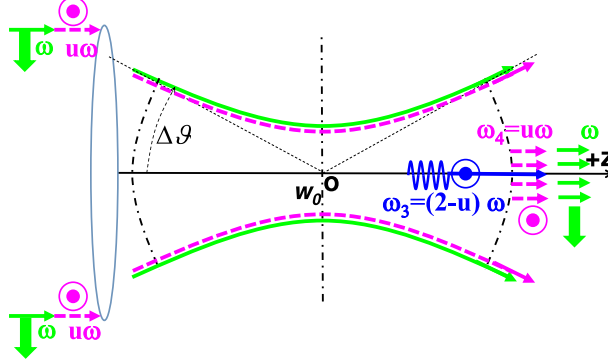


Fig. 6. A laser field with  $\omega$  (solid line) mixed with an *inducing* laser field with  $u\omega$  (dashed line) is focused simultaneously. The photon with  $\omega_4 = u\omega$  is induced to be created from the sea of photons. Simply due to the energy-momentum conservation law,  $\omega_3$  is then *enforced* to be  $(2-u)\omega$  in the forward direction as shown in Fig. 2. We re-emphasize that  $p_4$  had been chosen precisely for this purpose. We also point out that  $p_3$  is included in none of the momentum ranges of the initial frequency-mixed lasers. In this way  $\omega_3$  remains to be a clear experimental signature by further requiring the proper polarization state.

We may argue, on the other hand, preparing another incident beam may provide another type of the 2-photon system with the frequencies  $\omega$  and  $\omega_4$ , coming to the interaction (3.1). Such a two-body system, however, makes a negligible contribution to the event rate, if only spontaneous processes are taken into account. In spite of all such unimportant contributions, we have demonstrated that adding the inducing beam as prescribed above does yield the frequency-upshifted photon, as was predicted without the inducing beam before, re-emerging simply with the rate enhanced to the level of physical detectability.

## §6. Conclusion

We are going to summarize briefly how we have arrived at the final scenario in which the gravitationally weak signals are enhanced to the level of being subject to measurements, hopefully in the realm of laboratory experiments, as will be shown according to the series of steps below.

(i) We exploited the resonance nature of the scalar field. We consider the cross section of elastic photon-photon scattering in the  $s$ -channel, exhibiting an overall behavior of  $\mathcal{O}(M_{\text{P}}^{-4})$ . At the resonance precisely corresponding to  $m_\phi$ , the cross section reaches the peak value of  $\mathcal{O}(M_{\text{P}}^0)$ , independent of the strength of the force. In this sense we expect an enhancement of the size  $\mathcal{O}(M_{\text{P}}^4)$ , which might be re-expressed by a dimensionless parameter  $(M_{\text{P}}/m_\phi)^4 \sim (10^{36})^4 \sim 10^{144}$ . This advantage can be offset by the width  $a \sim 10^{-77}(\text{eV})^2$ , being extremely narrower than any of the realistic squared-energy scales, chosen to be  $\sim (\text{eV})^2$ , for example.

We then apply certain averaging process over the practical range, as noted above. This causes a setback of the enhancement of  $\sim 10^{-77}$ , which leaves us nearly a half-way, still above the bottom by more than 70 orders of magnitude.

(ii) Both of the phase-volume integral and the flux of the photons in the quasi-parallel frame result in the enhancement  $\sim \vartheta^{-2}$ , where  $\vartheta \sim 10^{-9}$  is for the half the angle made by the two incident photons. Out of the expected total amount  $\vartheta^{-4} \sim 10^{36}$ , a “half,”  $\vartheta^{-2} \sim 10^{18}$  was shown to be compensated by the small probability with which we detect the characteristic forward peak of the nearly frequency-doubled outgoing photon. The remaining  $\vartheta^{-2}$ , however, does contribute the enhancement by  $\sim 10^{18}$ .

(iii) We finally appealed to highly intensified laser beam, supposed to be described most likely by a coherent state providing with, not the vacuum, but a sea of photons which the incident or outgoing photons are annihilated into or created from. Due basically to the induced creation/annihilation mechanism, each of the amplitudes for three of the external photons is enhanced by  $\sqrt{N}$  with  $N$  for the average photon number contained in each of the pulse beam. The entire yield  $\mathcal{Y}$  per pulse focusing for observing the expected frequency-shifted photons in the forward direction is then proportional to  $N^3$ . We find that  $\mathcal{Y}$  turns out to be of the order unity if  $N$  is as large as  $10^{21}$ , corresponding fortunately to the beam supposed to be available soon with the most advanced laser technology.

Summarizing, we point out that we have achieved only what we may call a simplified overview of the whole proposal. In the future studies on the more realistic world, on the other hand, we should focus upon more details, particularly on how we depart from the single-frequency mode of the coherent state. This may result in revising the present estimate for the necessary energy per laser pulse to some extent, though the major conclusions reached so far are expected to remain basically unchanged.

### Acknowledgments

K. H. thanks D. Habs, R. Hörline, S. Karsch, T. Tajima, S. Tokita, L. Veisz and M. Zepf for valuable discussions. Y. F. is indebted to Y. Sakurayama, A. Iwamoto, T. Izuyama, H. Matsumoto and K. Shimizu for their helpful comments. This work was supported by the Grant-in-Aid for Scientific Research no.21654035 from MEXT of Japan in part and the DFG Cluster of Excellence MAP (Munich-Center for Advanced Photonics).

### Appendix A

#### — Phase-volume integral —

We start with

$$\frac{d\sigma}{d\Omega_3} = \frac{1}{64\pi^2} \frac{1}{\omega^2 \sin^2 \vartheta} \int_0^\infty d\omega_3 \omega_3 \int \frac{d^3 p_4}{2\omega_4} \delta^4(p_3 + p_4 - p_{\text{in}}) |\mathcal{M}|^2. \quad (\text{A.1})$$

We insert an identity

$$1 = \int_0^\infty dp_4^0 \delta(p_4^0 - \omega_4) = \int_{-\infty}^\infty dp_4^0 2\omega_4 \delta(p_4^2) \Theta(p_4^0), \quad (\text{A.2})$$

where  $\omega_4 > 0$  is always understood in what follows.

In the quasi-parallel frame, we compute

$$\begin{aligned} p_4^2 &= (p_1 + p_2 - p_3)^2 = 2p_1p_2 - 2p_3(p_1 + p_2) \\ &= 4\omega(1 - \cos\vartheta \cos\theta_3) \left( \omega_3 - \omega \frac{\sin^2\vartheta}{1 - \cos\vartheta \cos\theta_3} \right), \end{aligned} \quad (\text{A.3})$$

hence

$$\delta(p_4^2) = \frac{1}{4\omega(1 - \cos\vartheta \cos\theta_3)} \delta(\omega_3 - \hat{\omega}_3), \quad (\text{A.4})$$

where

$$\frac{\hat{\omega}_3}{\omega} \equiv \frac{\sin^2\vartheta}{1 - \cos\vartheta \cos\theta_3}. \quad (\text{A.5})$$

By re-expressing this into

$$\frac{1}{1 - \cos\vartheta \cos\theta_3} \approx \vartheta^{-2} \frac{\hat{\omega}_3}{\omega}, \quad (\text{A.6})$$

which is substituted into (A.4), further into (A.1) through (A.2), we finally obtain

$$\frac{d\sigma}{d\Omega_3} = \frac{1}{64\pi^2\omega^2} \vartheta^{-2} \int d\omega_3 \omega_3 \frac{\hat{\omega}_3}{4\omega^2} \vartheta^{-2} \delta(\omega_3 - \hat{\omega}_3) |\mathcal{M}|^2 = \frac{1}{64\pi^2\omega^2} \vartheta^{-4} \left( \frac{\hat{\omega}_3}{2\omega} \right)^2 |\mathcal{M}|^2, \quad (\text{A.7})$$

where  $\omega_3$ , if contained in  $|\mathcal{M}|^2$ , is understood to be  $\hat{\omega}_3$ , though such  $\omega_3$ -dependence rarely occurs in practice.

We also point out that the invariant amplitude is supposed to represent the effect of the  $\phi$  resonance. Particularly used in conjunction with the averaging process explained in section 3,  $|\mathcal{M}|^2$  is nonzero only for the specific choices of the initial frequency or the incident angle favoring the resonance condition. In this sense the purely kinematical contribution represented by the terms other than  $|\mathcal{M}|^2$  in (A.7) will be important.

## Appendix B

— An estimate of the coefficient  $\eta$  —

By substituting  $\vartheta_\pm$  in LHS of (3.15), we obtain

$$\pm \tilde{a} = \chi(\vartheta_\pm) = \omega_1^2 K_\pm, \quad (\text{B.1})$$

$$K_\pm = 1 - \left( \frac{\vartheta_r}{\vartheta_\pm} \right)^2, \quad (\text{B.2})$$

By identifying LHS of (B.1) with  $\pm a\eta$ , we also obtain

$$\eta = \pm \eta_0 K_\pm, \quad (\text{B.3})$$

where  $\eta_0$  is already defined by (3.19), also  $\kappa \equiv B^2/(4\pi) \sim 10^{-5}$ . Notice that (B.3) consists of the two equations including the equality

$$K_+ = -K_-, \quad (\text{B.4})$$



a manifestation of the assumed symmetry for simplicity, the same distances of  $\chi$  from the resonance at  $\chi = 0$  in the integration range in (3.11). Using this in (B.3), produces

$$\eta = \eta_0 \frac{1}{2} (K_+ - K_-) = \eta_0 \frac{1}{2} \left( \left( \frac{\vartheta_r}{\vartheta_-} \right)^2 - \left( \frac{\vartheta_r}{\vartheta_+} \right)^2 \right). \quad (\text{B.5})$$

We also substitute (B.2) into (B.4), obtaining

$$\left( \frac{\vartheta_r}{\vartheta_+} \right)^2 + \left( \frac{\vartheta_r}{\vartheta_-} \right)^2 = 2. \quad (\text{B.6})$$

By eliminating  $\vartheta_-$  from (B.5) and (B.6), we finally obtain

$$\eta = \left( 1 - \left( \frac{\vartheta_r}{\vartheta_+} \right)^2 \right) \eta_0, \quad (\text{B.7})$$

hence deriving (3.18).

### Appendix C

— Averaging over  $\vartheta$  —

We consider

$$\overline{|\mathcal{M}_{1111s}|^2}_{\vartheta} = \frac{\mathcal{N}_{\vartheta}}{\mathcal{D}_{\vartheta}}, \quad (\text{C.1})$$

where

$$\mathcal{N}_{\vartheta} = \int_{\vartheta_-}^{\vartheta_+} |\mathcal{M}_{1111s}|^2 d\vartheta, \quad \text{and} \quad \mathcal{D}_{\vartheta} = \vartheta_+ - \vartheta_-. \quad (\text{C.2})$$

On RHS of the first of (C.2), we substitute the Jacobian  $J$  to obtain

$$d\vartheta = J d\chi, \quad (\text{C.3})$$

where

$$J = \left( \frac{d\vartheta}{d\chi} \right) = \left( \frac{d\chi}{d\vartheta} \right)^{-1} = \frac{\vartheta^3}{2\omega_1^2 \vartheta_r^2}, \quad (\text{C.4})$$

as has been obtained from (3.15). We substitute (C.3) into (3.11), in which the integrand is dominated by the value at  $\chi = 0$ , corresponding to  $\vartheta = \vartheta_r$  according to (3.15). We then find that RHS of  $\mathcal{N}_{\vartheta}$  in the first of (C.2) is  $\vartheta_r / (2\omega_1^2)$ , the value of (C.4) at  $\vartheta = \vartheta_r$ , times the value on RHS of  $2\tilde{a} \overline{|\mathcal{M}_{1111s}|^2}$ . In this way we obtain

$$\frac{\overline{|\mathcal{M}_{1111s}|^2}_{\vartheta}}{\overline{|\mathcal{M}_{1111s}|^2}} \approx \frac{1}{\mathcal{D}_{\vartheta}} \frac{\vartheta_r}{2\omega_1^2} 2\tilde{a} \approx \frac{\vartheta_r}{\vartheta_+}, \quad (\text{C.5})$$

where we have used  $\mathcal{D} \approx \vartheta_+$ , as well as

$$\tilde{a} = a\eta \approx a\eta_0 = \omega_1^2, \quad (\text{C.6})$$

in accordance with (3.19).

### Appendix D

— Partially integrated cross section,  $\bar{\sigma} \sim \vartheta^{-2}$  —

From (2.5) and (2.6), we derive

$$\int_0^{\bar{\theta}_3} \left(\frac{\bar{\omega}_3}{2\omega}\right)^2 \sin \theta_3 d\theta_3 = \frac{\vartheta^4}{4} \int_{\underline{x}}^1 (1 - x \cos \vartheta)^{-2} dx \equiv \frac{\vartheta^4}{4} \int_{\underline{x}}^1 f(x) dx, \quad (\text{D.1})$$

where  $f(x)$  has its indefinite integral, such that  $f = d\mathcal{F}/dx$  with  $x = \cos \theta_3$ ;

$$\mathcal{F}(x) = \frac{1}{\cos \vartheta} (1 - x \cos \vartheta)^{-1} \approx (1 - x \cos \vartheta)^{-1}, \quad (\text{D.2})$$

with  $\cos \vartheta \sim 1$  in the denominator since the correction term  $\sim \vartheta^2$  has been already in (D.1) as a multiplicative factor. We readily find

$$(\text{D.1}) = \frac{\vartheta^4}{4} (\mathcal{F}(1) - \mathcal{F}(\underline{x})) \approx \frac{\vartheta^4}{4} \vartheta^{-2} \left(2 - \frac{\bar{\omega}_3}{\omega}\right) = \frac{1}{4} \vartheta^2 u, \quad (\text{D.3})$$

thus yielding (4.4), where (D.2), (A.6) with  $\theta_3, \hat{\omega}_3$  replaced by  $\bar{\theta}_3, \bar{\omega}_3$ , respectively, and (4.2) have been used. This provides us with (4.4).

For a certain experimental condition, we may need the integral in (D.1), but with the lower bound 0 replaced by  $\underline{\theta}_3$ . In order to estimate  $\mathcal{F}(x)$  in a more general value of  $x$ , we find it convenient to introduce  $v_3$  by

$$\theta_3 = v_3 \vartheta, \quad \text{hence} \quad u = 2v_3^2. \quad (\text{D.4})$$

We then obtain

$$\begin{aligned} \mathcal{F}(x) &\approx (1 - x \cos \vartheta)^{-1} = \left(1 - \left(1 - \frac{1}{2} v_3^2 \vartheta^2\right) \cos \vartheta\right)^{-1} \\ &= \left(1 - \cos \vartheta + \frac{1}{2} v_3^2 \vartheta^2 \cos \vartheta\right)^{-1} \approx \left(\frac{1}{2} \vartheta^2 + \frac{1}{2} v_3^2 \vartheta^2 \cos \vartheta\right)^{-1} \\ &= \left(\frac{1}{2} \vartheta^2 (1 + v_3^2)\right)^{-1} = 2\vartheta^{-2} \frac{1}{1 + v_3^2} \approx 2\vartheta^{-2} (1 - v_3^2). \end{aligned} \quad (\text{D.5})$$

According to (D.1) we find

$$\bar{\sigma} = \frac{\pi^2}{16\omega^2} \eta^{-1} (\mathcal{F}(\underline{x}) - \mathcal{F}(\bar{x})) \approx \frac{\pi^2}{16\omega^2} \eta^{-1} 2\vartheta^{-2} (\bar{v}_3^2 - \underline{v}_3^2). \quad (\text{D.6})$$

### Appendix E

— Understanding the enhanced yield in the quasi-parallel frame —

The cross section  $\bar{\sigma}$  is very large due to the factor  $\sim \vartheta^{-2} \sim 10^{18}$  in (4.5), making a significant contribution to the value of the final yield  $\mathcal{Y}$  according to (5.13). We should make sure, however, that the calculation correctly ensures that we avoid to fall into the same path as another example of  $\vartheta^{-2}$  which was shown to be compensated away by a small partially-integrated cross section discussed toward the end of section 4. For this purpose, it might be helpful if we better understand how the relation (5.13) is derived applied particularly to

scattering of coherent states. The argument will be made most conveniently by identifying the enhancement  $\sim \vartheta^{-2}$  under discussion to come from the flux in computing the elastic photon-photon scattering cross section in the quasi-parallel incident frame.

We start with explaining how we compute the flux in the photon-photon scattering cross section based on Møller's formulation which may be found in (8-50) of,<sup>20)</sup> or (3.78) of.<sup>21)</sup>

Define a Lorentz-invariant function

$$F = \sqrt{(p_1 p_2)^2 - m^4}, \quad (\text{E.1})$$

for two identical massive particles of the momenta  $p_1$  and  $p_2$ . We may demonstrate that (E.1) is justified in the number of well-known examples.

First in the center-of-mass frame with  $\vec{p}_1 = -\vec{p}_2 = \vec{p}$ ,  $p_1^0 = p_2^0 = \omega$ , we derive easily  $F = \omega^2 v_{\text{rel}}$ , where  $\vec{v}_{\text{rel}} = \vec{v}_1 - \vec{v}_2 = 2\vec{p}/\omega$ , with  $\vec{v}_i = \vec{p}_i/\omega$  ( $i=1,2$ ).

Likewise, in the laboratory frame we have  $\vec{p}_1 = \vec{p}, \omega_1 = \omega$ , and  $\vec{p}_2 = 0, \omega_2 = m$ , from which follows  $F = m\omega_1 v_1 = m\omega_1 v_{\text{rel}}$ .

These exercises indicate a computational rule that the familiar normalization factor  $(\omega_1 \omega_2)^{-1}$  also divided by  $v_{\text{rel}}$  should be replaced by a Lorentz-invariant factor  $F^{-1}$ .

Now we go to the massless limit  $m \rightarrow 0$  in (E.1). In the "center-of-mass" frame with  $\vec{p}_2 = -\vec{p}_1, \omega_2 = \omega_1$ , we compute

$$|p_1 p_2| = |-\vec{p}_1^2 - \omega_1^2| = 2\omega^2 = \omega^2 \times (1 + 1), \quad (\text{E.2})$$

where we interpret  $(1 + 1 = 2)$  reasonably as the relative velocity of the massless particles. After these preparations, we finally consider the quasi-parallel geometry as was discussed in section 2;

$$\vec{p}_{2x} = -\vec{p}_{1x}, \quad \vec{p}_{2z} = \vec{p}_{1z}, \quad \omega_2 = \omega_1, \quad (\text{E.3})$$

from which follows immediately

$$F = |p_1 p_2| = |-\omega^2 \sin^2 \vartheta + \omega^2 \cos^2 \vartheta - \omega^2| = \omega^2 | -2 \sin^2 \vartheta | = \omega^2 2 \sin^2 \vartheta, \quad (\text{E.4})$$

establishing what should be re-interpreted as the relative velocity in the present frame is given by  $2 \sin^2 \vartheta \sim 2\vartheta^2$ .

Usually the cross section obtained for a unit flux is multiplied with another flux to be determined depending on the physical circumstance. In the current beam-type experiment, as illustrated in Fig. 5, the photons are supplied from the left in the positive direction of the horizontal  $z$ -axis. This remains true even for two incident photons which will be bent afterward by the lens. In this sense we have no relative velocity prepared at the observational entrance doorway.

We then naturally adopt the equivalent concept of a "flow," which shares the same property with a flux; the number of particles passing through unit perpendicular area per unit time, but without relying on the relative velocity. The area perpendicular to the flow is chosen to be  $\pi w_0^2$ , where  $w_0$  is the waist of the laser beam. We notice a decisive difference from the way we defined the flux in the microscopic range in which the relative velocity is obviously perpendicular to the  $z$ -axis. We find no way for the two ways to affect each other.

A crucial observation is that by particles mentioned above we never mean the individual photons which are uncountable, but should understand to be the coherent states described by (5.2). The flow thus represents the number of these coherent states per perpendicular area per unit time. We prepared the initial state as a single number of the coherent state, with the response to the scalar field interaction basically given by (5.7).

We also notice that we are going to estimate the yield per pulse focusing, instead of the rate per unit time. We are integrating the flow over the entire time-span of the pulse, giving the number unity for the coherent state. This is the way we obtained  $I_c$  by a product of unity times  $N^2$  in (5.14).

After all we are left with none of the variables responsible for any of the time-dependence, like the flow, leading to the simple result (5.13) with (5.14), in which the large value coming from  $\vartheta^{-2}$  in  $\bar{\sigma}$  is robust.

### References

- 1) A.G. Riess, et al, *Astron. J.* **116** (1998), 1009, S. Perlmutter, et al, *Nature* **391**, (1998), 51.
- 2) R. R. Caldwell, et al, *Phys. Rev. Lett.* **80** (1998), 1582. L. Wang, et al, *Astrophys. J.* **530** (2000), 17. S. Tsujikawa, arXiv:1004.1493.
- 3) Y. Fujii and K. Maeda, *The Scalar-Tensor Theory of Gravitation* (Cambridge Univ. Press, 2003).
- 4) L. Amendola and S. Tsujikawa, *Dark Energy: Theory and Observations* (Cambridge Univ. Press, 2010).
- 5) P. Jordan, *Schwerkraft und Weltall* (Friedrich Vieweg und Sohn, Brunschweig, 1955).
- 6) Y. Fujii, *Phys. Rev.* **D26** (1982), 2589. O. Bertolami, *Nuovo Cimento* **93** (1986), 36.
- 7) Y. Fujii, *Prog. Theor. Phys.* **181** (2007), 983.
- 8) K. Maeda and Y. Fujii, *Phys. Rev.* **D79** (2009), 084026. Y. Fujii, arXiv:0908.4324 [astro-ph.CO]. Y. Fujii, Proc. IAU 2009 JD9, 03-14 Aug. 2009, Mem. S.A.It. Vol. 75, 282, arXiv:0910.5090 [astro-ph.CO].
- 9) Y. Fujii, Proc. The 20th Workshop on General Relativity and Gravitation, 21-25 Sept. 2010, Kyoto. <http://www2.yukawa.kyoto-u.ac.jp/~jgrg20/proceedings> 108.
- 10) Y. Fujii, *Nature Phys. Sci.* **234** (1971), 5; *Ann. Phys. (N. Y.)* **69** (1972), 494.
- 11) See, for example, Figures; 2.13, 4.16-17 in E. Fischbach and C. Talmadge, *The Search for Non-Newtonian Gravity* (AIP Press, Springer-Verlag, N.Y., 1998). See also S. Schlamminger et al, *Phys. Rev. Lett.* **100** (2008), 041101, and papers cited therein.
- 12) Y. Fujii and M. Sasaki, *Phys. Rev.* **D75** (2007), 064028.
- 13) For the proposed laser-related experiments, see, for example, G. Mueller, P. Skivie, D.B. Tanner and Karl van Bibber, arXiv: 0907.5387. A. Lindner, arXiv:0910.1686.
- 14) See Equation (5.11) in W. Dittrich and H. Gies, *Probing the Quantum Vacuum* (Springer 2007).
- 15) J. D. Bekenstein, *Phys. Rev.* **D25** (1982), 1527.
- 16) C. Brans and R. H. Dicke, *Phys. Rev.* **124** (1961), 925.
- 17) R. J. Glauber, *Phys. Rev.* **131** (1963), 2766.
- 18) C. Itzykson and J. Zuber, *Quantum Field Theory* (New York McGraw-Hill Book Co., 1985)
- 19) Amnon Yariv, *Optical Electronics in Modern Communications* (Oxford University Press, Inc. 1997).
- 20) J. M. Jauch and F. Rhorlich, *The theory of photons and electrons*, (Addison-Wesley, 1954).
- 21) W. Greiner and J. Reinhardt, *Quantum Electrodynamics*, (Springer 1994).